Preliminary analysis of polarization effects in bent uncoupled-core multicore fibers

Cappelletti, Martina; Orsuti, Daniele; Vandborg, Mads Holmark; Aitkulov, Arman; Del Olmo, Pablo; Schenato, Luca; Magarotto, Mirko; Santagiustina, Marco; Antonelli, Cristian; Mecozzi, Antonio

Total number of authors:
16

Published in:
Proceedings of 28th International Conference on Optical Fiber Sensors

Publication date:
2024

Document Version
Peer reviewed version

Preliminary analysis of polarization effects in bent uncoupled-core multicore fibers

**Martina Cappelletti,[1,*], Daniele Orsuti,[1] Mads Holmark Vandborg,[2,1]
Arman Aitkulov,[1] Pablo Del Olmo,[1] Luca Schenato,[1], Mirko Magarotto,[1]
Marco Santagiustina,[1] Cristian Antonelli,[3] Antonio Mecozzi,[3] Tetsuya Hayashi,[4]
Lars Grüner-Nielsen,[2] Lars Søgaard Rishøj,[2] Karsten Rottwitt,[2]
Andrea Galtarossa,[1] and Luca Palmieri[1]**

[1]*Department of Information Engineering, University of Padova, Via G. Gradenigo 6/B, Padova, Italy*
[2]*Technical University of Denmark, Ørsteds Plads 343, 2800 Kgs. Lyngby, Denmark*
[3]*Department of Physical and Chemical Sciences, University of L'Aquila, 67100 L'Aquila, Italy*
[4]*Optical Communications Laboratory, Sumitomo Electric Industries, Ltd., Yokohama 244-8588, Japan*

[*]*martina.cappelletti.1@phd.unipd.it*

Abstract: Uncoupled-core multicore fibers are becoming popular tools for many fields including optical fiber sensing. We analyze for the first time the polarization effects that take place when these fibers are bent.

1. Introduction

In recent years, there has been extensive research on uncoupled-core multi-core fiber (UMCF) as a solution to address the impending capacity crunch in optical fiber communication systems [1]. Unlike traditional single mode fiber (SMF), UMCF incorporates multiple cores within a single fiber cladding, enabling parallel transmission paths along a single fiber and significantly enhancing the transmission capacity. These advantages have spurred significant improvements in the production processes of UMCF, which can now be drawn in spans of tens of kilometers with telecom-quality grade [2]. The unique structure of UMCFs has led to significant research efforts in their application also in fields beyond telecommunication, such as microwave photonics [3] and optical sensing. Most noticeably, UMCF are intensely investigates as a tool for bending and shape sensing [4–8], but also for measuring temperature, torsion and refractive index [9–11]. Moreover, some studies have explored the use of UMCF to enable discriminative measurements of temperature and strain [12].

Despite this wide interest in UMCFs, their polarization properties are still largely unexplored. Very recent preliminary investigations [13] have shown that the UMCF's cores are characterized by a very ordered birefringence, with mild strength in the range of a few rad/m. This characteristic make UMCFs an ideal technological platform for distributed polarization sensing. To this aim, however, the effects that fiber manipulation (namely, bending, twist, compression, etc.) may have on its birefringence have to be fully understood. In this study, we present a preliminary theoretical and experimental analysis of the effects that bending has on the birefringence of MCFs' cores. We show that in UMCFs bending birefringence scales proportionally to the square of the applied curvature as in SMF, yet the proportionality coefficient depends on the core position with respect to the bending axis.

2. Theoretical model of bending effects

When a cylindrical bar like an optical fiber is bent, a complex stress field builds up across its section, which is made of two main contributions [14]. The first one is a longitudinal component, σ_z, oriented along the fiber axis, and related to the elongation (compression) that the outer (inner) portion of the bent fiber experiences. This stress component varies along the direction of the curvature vector as $\sigma_z = \kappa E x$, where $\kappa = 1/R_B$ is the curvature, R_B the bending radius and $E \approx 72\,\text{GPa}$ the Young modulus of fused silica (see Fig. 1(a)). The second component is related to the pressure that the bend layers of the fiber exert toward its center. As a result, this stress is oriented along the curvature axis and it is given by $\sigma_x = \kappa^2 (E/2)(x^2 - R_{CL}^2)$, where R_{CL} is the radius of the cladding (see Fig. 1(b)). Owing to the elasto-optic effect, these stress fields cause variations of the relative dielectric tensor of the fiber glass given, respectively, by $\delta\varepsilon_z = -\kappa n^4 x\,\text{diag}(c_1, c_1\,c_2)$ and $\delta\varepsilon_x = -\frac{1}{2}\kappa^2 n^4 (x^2 - R_{CL}^2)\,\text{diag}(c_2, c_1\,c_1)$ where n is the average refractive index, $\text{diag}(\cdot)$ indicate a diagonal matrix, and $c_1 \approx 0.206$ and $c_2 \approx 0.032$ are coefficients related to the elasto-optic properties of fused silica [15]. These dielectric perturbations induce coupling among the light modes propagating in each core of an UMCF, which can be described in terms of the coupling coefficients

$$K_{\mu,\nu} = \iint_S \vec{E}_\mu^* (\delta\varepsilon_z + \delta\varepsilon_x) \vec{E}_\nu \, dx' dy' \,, \tag{1}$$

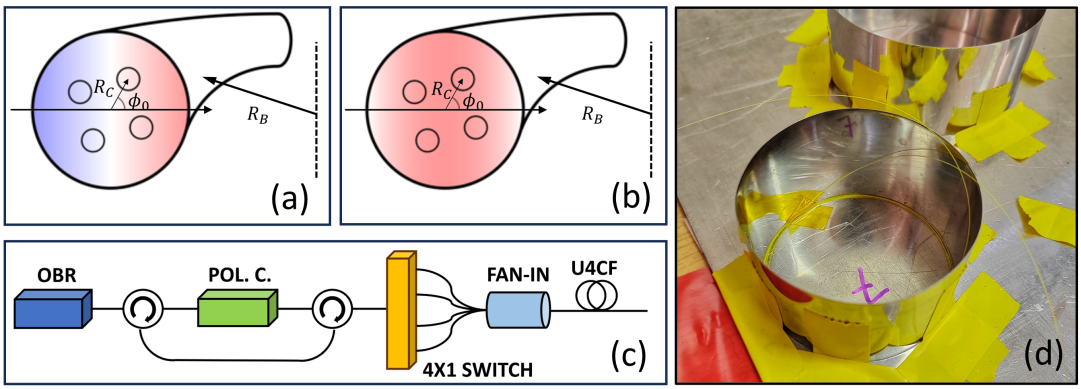

Fig. 1. Schematic of the longitudinal (a) and compressive (b) stress components. (c) Experimental setup for sequential interrogation of the cores for different input SOPs. (d) Picture illustrating the bending of the MCF within a cylindrical shape with a diameter of 7 cm.

where $\vec{E}(x',y')$ is the field distribution of the modes with respect to the reference frame $\{x',y'\}$ centered on the core. In the case of UMCFs, however, the cores are not centered with respect to the fiber, so the dielectric perturbations must be evaluated in $x = x' - x_0$, where x_0 is the lateral offset of the core. Referring to Figs. 1(a-b), we can write $x_0 = R_C \cos\phi_0$, highlighting the fact that bending effects in UMCF depend on the fiber orientation with respect to the bending axis.

Direct inspection of (1) shows that, owing to the symmetry of the fundamental mode, the longitudinal stress σ_z does not have any mode-coupling effect, regardless of the core position. On the contrary, the transverse stress σ_x causes bending birefringence. Just as in SMFs, this birefringence is proportional to the square of the curvature and its fast axis is orthogonal to the bending axis. Differently from SMFs, however, the strength of this bending birefringence varies with the core position according to:

$$\beta_{bend} \approx 0.273(n^3/\lambda)\left(R_{CL}^2 - R_C^2\cos^2\phi_0\right)\kappa^2 . \tag{2}$$

In the following section we report experimental results supporting this model.

3. Experimental analysis

To test the above theoretical model, we have used polarization sensitive reflectometry (PSR) [16] to measured the birefringence vector of the cores, under different bend conditions. Figure 1(c) shows the experimental setup, which comprises a polarization-sensitive OFDR (Luna Innovations OBR 4600) and a polarization controller (Agilent 11896A) to change the input state of polarization (SOP). To enable independent examination of the fiber cores without perturbing the fiber, a 1×4 optical switch is employed. Access to the MCF is achieved through the Opto-scribe 3D Optofan series fan-in module. The UMCF used in the experiment is an uncoupled-4-core fiber (U4CF), described in details in Ref. [17]. The birefringence vector is measured along each core according to the method described in Ref. [16]. Initially, a reference measurement is taken when the UMCF is straight. Subsequently, the measurements are repeated after the last three meters of the fiber are carefully wound inside cylinders of different radii (see Fig. 1(d)), namely 5 cm, 3.5 cm, 3 cm, 2.5 cm, and 1.9 cm.

While the winding has been performed with care, trying to avoid twisting the fiber as much as possible, the experimental procedure is hindered by the fact that the core positions are not known neither when the fiber is straight, nor after the winding. We take into consideration this fact by considering the following model. When the fiber is straight, free of any bending, the birefringence vector measured in each core can be expressed as

$$\vec{\beta}_{S,n}(z) = \beta_{int,n}(z)\mathbf{R_3}\big((2-g)\tau_0(z) + 2\psi_n(z)\big)\,\hat{s}_1 , \tag{3}$$

where $\beta_{int,n}(z)$ and $\psi_n(z)$ are the strength and orientation of the intrinsic birefringence of the nth core, and $\tau_0(z)$ is any twist possibly applied to the straight fiber; note that this is of course common to every core. The matrix $\mathbf{R_3}(\theta)$ represents rotation by an angle θ around the axis $(0,0,1)^T$. Note also that in writing (3), we considered the fact that PSR measurement returns linear birefringence by construction, and any circular birefringence due to the torsion τ_0 appears as a further rotation by $-g\tau_0$, with $g \approx 0.15$ [18]. After the fiber is bent, the total measured birefringence is equal to the vector sum of the intrinsic one and the bend-induced one, all rotated by the apparent factor $-g\tau_B(z)$ due to any twist induced during the winding. In formulas, the birefringence vector measured along the nth core after the winding reads

$$\vec{\beta}_{M,n}(z) = \beta_{int,n}\mathbf{R_3}\big((2-g)(\tau_0-\tau_B) + 2\psi_n\big)\,\hat{s}_1 + \beta_{bend,n}\mathbf{R_3}\big(-g(\tau_0-\tau_B)\big)\hat{s}_1 . \tag{4}$$

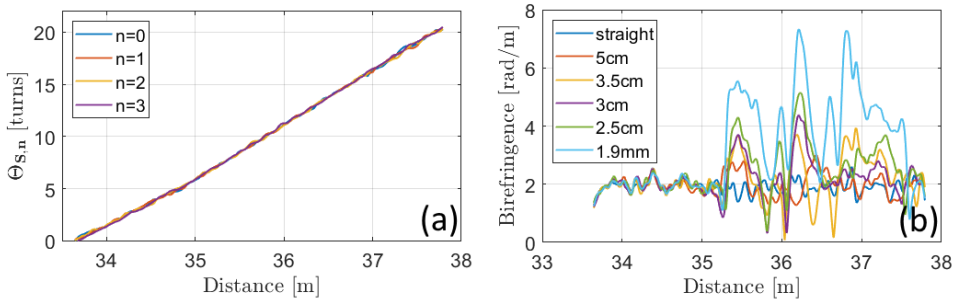

Fig. 2. (a) Angle of birefringence measured for all the cores when the fiber is laid straight (b) Modulus of birefringence, for one core, in straight configuration and when the last 2 meters are coiled with different radii.

The bending axis in our experiment is fixed, and this, without loss of generality, lets us assume that the bending birefringence is constantly oriented along $\hat{s}_1$. The matrix $\mathbf{R_3}(-g(\tau_0-\tau_B))$ accounts for the apparent rotation due to circular birefringence. The quantities τ_0, τ_B, and ψ_n are unknown; nevertheless, the measurements of $\vec{\beta}_{S,n}$ on the straight fiber allow to calculate the angles $\theta_{S,n}(z) = (2-g)\tau_0(z) + 2\psi_n(z)$ up to an unknown constant [16]. The results are shown in Fig. 2(a), and clearly show that the intrinsic birefringence orientation varies in the same way in every core. This is consistent with the hypothesis that this intrinsic birefringence is due to a common stress field induced during the drawing with an axial symmetry around the fiber axis [13]. Because of this, we set the birefringence orientation in each core equal to $\psi_n(z) = \psi_0(z) + n\pi/2$, with $n = 0,1,2,3$ indicating the cores counted in clockwise direction. Similarly, the bending birefringence in each core is equal to $\beta_{bend,n} \approx 0.273(n^3/\lambda)(R_{CL}^2 - R_C^2\cos^2(\phi_0 + n\pi/2))\kappa^2$, where ϕ_0 accounts for the unknown absolute orientation of the cores. Figure 2(b) shows, as an example, the modulus of $\vec{\beta}_{M,n}(z)$ for different bending radii, including the straight fiber, measured on a specific core ($n = 2$). We clearly see that the bending (which starts from about 35 m) has a dramatic effect on the birefringence strength and, despite the applied curvature is constant, this effect is largely varying along the fiber, just because of the varying orientation of the cores.

To get rid of the effect of the unknown angles, we consider the quantities $p_{1,n}(z) = (\vec{\beta}_{M,n} \cdot \vec{\beta}_{S,n})/\beta_{int,n}$ and $p_{2,n}(z) = \{\vec{\beta}_{M,n} \times \vec{\beta}_{S,n}\}_3/\beta_{int,n}$, where by $\{\cdot\}_3$ we indicate the third component of the vector; note that these can be calculated from the experimental data. Afterwards, from these we calculate the quantities

$$q_1(z) = (p_{1,0} + p_{1,2}) - (p_{1,1} + p_{1,3}) = \gamma_1 \cos((g-2)\tau_b) + \gamma_2 \kappa^2 \cos(2(\tau_0 + \psi_0) + g\tau_b), \quad (5)$$

$$q_2(z) = (p_{2,0} + p_{2,2}) - (p_{2,1} + p_{2,3}) = \gamma_1 \sin((g-2)\tau_b) + \gamma_2 \kappa^2 \sin(2(\tau_0 + \psi_0) + g\tau_b) \quad (6)$$

where the final expressions are reached by explicit calculation, with $\gamma_1 = \beta_{int,0} - \beta_{int,1} + \beta_{int,2} - \beta_{int,3}$ and $\gamma_2 \approx 0.546(n^3/\lambda)(2R_{CL}^2 - R_C^2)$. For the fiber at hand $R_{CL} \approx 62.5\,\mu$m, $R_C \approx 28.4\,\mu$m, and $n \approx 1.466$; hence, for $\lambda = 1550\,$nm we find $\gamma_2 \approx 7.8\,$mm. Note that due to the already mentioned symmetry in the intrinsic birefringence of the UMCF, each core has almost the same birefringence strength (as verified experimentally from the measures of $\vec{\beta}_{S,n}$); therefore, the quantity γ_1 is quite small and in (5) and (6) we can set $\gamma_1 \approx 0$. As a consequence, we can finally calculate the quantity $B(z) = (q_1^2(z) + q_2^2(z))^{1/2} \approx \gamma_2 \kappa^2(z)$, which is independent of the unknown angles and is proportional to the squared curvature.

Figure 3(a) shows the values of $B(z)$ calculated for different winding radii. We see that up to about 35 m, where the fiber was not bent, $B(z)$ is almost zero as expected. Differently, in the bent region B increases with the applied curvature. The measured values show some fluctuations, which we ascribe to the approximation $\gamma_1 \approx 0$ and to some winding loops not perfectly deployed. Figure 3(b) shows the mean value of $B(z)$ in the bent region as a function of the squared curvature, κ^2. Markers refers to experimental data, whereas the continuous line is the linear fitting, showing that indeed the birefringence induced by bending an UMCF scales with the squared curvature. The fitting coefficient is 6.0 mm, somewhat off with respect to the expected one, likely because of nonperfect winding. Yet, the good fitting of the model with the experimental data implicitly confirms the dependence of the bending birefringence from the squared curvature and the core position in agreement with (2).

4. Conclusions

We have presented a theoretical model of polarization effects in uncoupled-core multicore fibers and supported it be preliminary experimental results. The results show that in UMCFs the bending birefringence scales with the squared curvature, as in SMFs. Differently from SMFs, however, the birefringence strength depends on the core

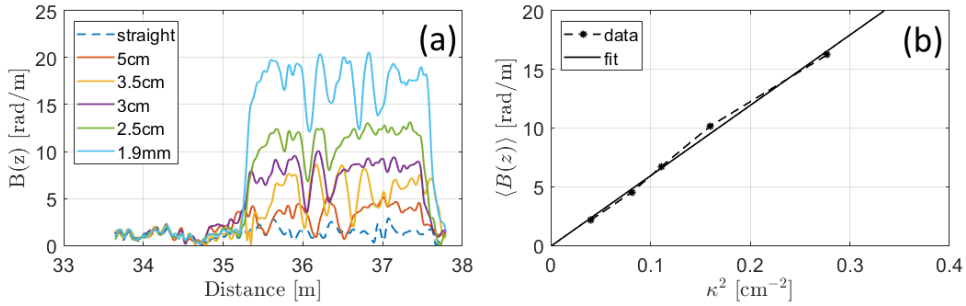

Fig. 3. (a) Plots of B(z) for different bending radii. (b) Average value of B(z) as a function of the squared curvature (markers: experimental data; solid line: linear fit).

position and hence is influenced by how the UMCF is twisted. This findings can have applied to a better modelling and understanding of MCF-based sensors and can pave the way to the use of UMCF as a sensing platform for distributed polarization sensing.

This work received partial support from the European Union under the Italian National Recovery and Resilience Plan (NRRP) of NextGenerationEU, partnership on "Telecommunications of the Future" (PE0000001 - program "RESTART") and MIUR (PRIN 2017, project FIRST).

References

1. P. J. Winzer, "Making spatial multiplexing a reality," Nat. Photonics **8**, 345–348 (2014).
2. T. Hayashi, "Multi-core fiber technology from design to deployment," in *2022 European Conference on Optical Communication (ECOC),* (IEEE, 2022), pp. 1–4.
3. I. Gasulla and J. Capmany, "Microwave photonics applications of multicore fibers," IEEE Photonics J. **4**, 877–888 (2012).
4. I. Floris, J. M. Adam, P. A. Calderón, and S. Sales, "Fiber optic shape sensors: A comprehensive review," Opt. Lasers Eng. **139**, 106508 (2021).
5. M. Cappelletti, A. Aitkulov, D. Orsuti, L. Schenato, M. Santagiustina, M. Magarotto, C. Antonelli, A. Galtarossa, A. Mecozzi, T. Hayashi, and L. Palmieri, "Fiber signature-domain multiplexing for high-speed shape sensing," in *European Workshop on Optical Fibre Sensors (EWOFS 2023),* vol. 12643 M. Wuilpart and C. Caucheteur, eds., International Society for Optics and Photonics (SPIE, 2023), p. 126431W.
6. A. Beisenova, A. Issatayeva, I. Iordachita, W. Blanc, C. Molardi, and D. Tosi, "Distributed fiber optics 3d shape sensing by means of high scattering np-doped fibers simultaneous spatial multiplexing," Opt. express **27**, 22074–22087 (2019).
7. P. S. Westbrook, T. Kremp, K. S. Feder, W. Ko, E. M. Monberg, H. Wu, D. A. Simoff, T. F. Taunay, and R. M. Ortiz, "Continuous multicore optical fiber grating arrays for distributed sensing applications," J. Light. Technol. **35**, 1248–1252 (2017).
8. Z. Zhao, M. A. Soto, M. Tang, and L. Thévenaz, "Distributed shape sensing using brillouin scattering in multi-core fibers," Opt. Express **24**, 25211–25223 (2016).
9. H. Du, H. Wu, Z. Zhang, C. Zhao, Z. Zhao, and M. Tang, "Single-ended self-calibration high-accuracy raman distributed temperature sensing based on multi-core fiber," Opt. Express **29**, 34762–34769 (2021).
10. G. Yin, L. Lu, L. Zhou, C. Shao, Q. Fu, J. Zhang, and T. Zhu, "Distributed directional torsion sensing based on an optical frequency domain reflectometer and a helical multicore fiber," Opt. Express **28**, 16140–16150 (2020).
11. Z. Zhu, D. Ba, L. Liu, L. Qiu, and Y. Dong, "Temperature-compensated distributed refractive index sensor based on an etched multi-core fiber in optical frequency domain reflectometry," Opt. letters **46**, 4308–4311 (2021).
12. M. A. S. Zaghloul, M. Wang, G. Milione, M.-J. Li, S. Li, Y.-K. Huang, T. Wang, and K. P. Chen, "Discrimination of temperature and strain in brillouin optical time domain analysis using a multicore optical fiber," Sensors **18** (2018).
13. R. Veronese, C. Antonelli, A. Mecozzi, T. Hayashi, M. Santagiustina, A. Galtarossa, and L. Palmieri, "Distributed measurement of birefringence in uncoupled multicore fibers," in *Optical Fiber Communication Conference,* (Optica Publishing Group, 2021), pp. W7B–3.
14. R. Ulrich, S. Rashleigh, and W. Eickhoff, "Bending-induced birefringence in single-mode fibers," Opt. letters **5**, 273–275 (1980).
15. L. Palmieri, "Coupling mechanism in multimode fibers," in *Next-Generation Optical Communication: Components, Sub-Systems, and Systems III,* vol. 9009 (SPIE, 2014), pp. 87–95.
16. L. Palmieri, "Distributed polarimetric measurements for optical fiber sensing," Opt. Fiber Technol. **19**, 720–728 (2013).
17. T. Hayashi, T. Nagashima, T. Nakanishi, T. Morishima, R. Kawawada, A. M. Antonio, and C. Antonelli, "Field-deployed multi-core fiber testbed," in *2019 24th OptoElectronics and Communications Conference (OECC) and 2019 International Conference on Photonics in Switching and Computing (PSC),* (2019), pp. 1–3.
18. A. Galtarossa, D. Grosso, and L. Palmieri, "Accurate characterization of twist-induced optical activity in single-mode fibers by means of polarization-sensitive reflectometry," IEEE Photonics Technol. Lett. **21**, 1713–1715 (2009).